CARBON letters

Note

Carbon Letters Vol. 17, No. 1, 65-69 (2016)

Cu nanoparticle-embedded carbon foams with improved compressive strength and thermal conductivity

Ji-Hyun Kim[1], Kyung Hoon Kim[1], Mi-Seon Park[1], Tae-Sung Bae[2,♣] and Young-Seak Lee[1,♣]

[1]Department of Applied Chemistry and Biological Engineering, Chungnam National University, Daejeon 34134, Korea
[2]Korea Basic Science Institute (KBSI), Jeonju 54907, Korea

Key words: pitch, nanoparticle, carbon foam, thermal conductivity, compressive strength

Article Info
Received 20 August 2015
Accepted 20 December 2015

***Corresponding Author**
E-mail: chemipia@kbsi.re.kr
youngslee@cnu.ac.kr
Tel: +82-63-270-3955
+82-42-821-7007

Open Access

DOI: http://dx.doi.org/10.5714/CL.2016.17.1.065

This is an Open Access article distributed under the terms of the Creative Commons Attribution Non-Commercial License (http://creativecommons.org/licenses/by-nc/3.0/) which permits unrestricted non-commercial use, distribution, and reproduction in any medium, provided the original work is properly cited.

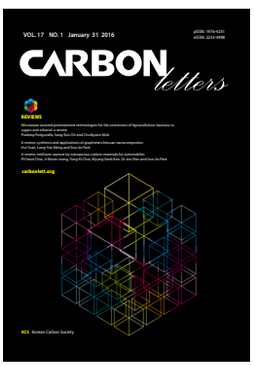

http://carbonlett.org

pISSN: 1976-4251
eISSN: 2233-4998

Copyright © Korean Carbon Society

Carbon foams (CFms) exhibit excellent physical properties, including good thermal conductivity, low density, high porosity and specific surface area, good vibration damping and shock absorption properties, and low thermal expansion coefficients. These properties are attractive in various applications such as thermal and electrical transfer devices, electrochemical supercapacitors, catalyst supports, gas adsorbents, filtration systems, and electromagnetic shielding. However, compared to metals and polymers, CFms do not exhibit good mechanical or thermal properties because of their porous structure; these shortcomings have limited the application of CFms in various fields [1-4].

Researchers have sought to improve the mechanical and thermal properties of CFms through the addition of carbon nanofibers, carbon nanotubes, graphite and metal plating [5,6]. CFms/copper composites were recently studied by Johnson et al. [7], who examined the thermal conductivity of wood-derived graphite and copper-graphite composites produced via electrodeposition. The thermal conductivity of the biomorphic graphite/copper composite was 10 times greater than that of biomorphic graphite, with the graphite/copper composites exhibiting a thermal conductivity ranging from 20 to 21 W/mK [7]. Zhai et al. [8] studied the effects of vacuum and ultrasonic co-assisted electroless copper plating on CFms and noted increased conductivity ranging from 700 to 1885.8 S/cm, and increased compressive strength ranging from 0.70 to 1.66 MPa with increasing copper content.

Cu exhibits high thermal and electrical conductivities, in the range of 350-400 W/mK and 59.17-59.59 × 10^6 $\Omega^{-1}m^{-1}$, respectively; and it can be adhesively bonded with carbon matrices such as carbon nanofoams, mesoporous carbon templates and nanotube/nanofiber assemblies through electrodeposition, electroless deposition, coating, and doping. Numerous researchers have reported that, when used as battery electrodes, metal-bonded carbon matrices exhibit high electrical capacity and increased oxidative stability compared to non-treated graphite foams [5,9-15]. However, preparing CFms with copper presents various problems. The coating of metal to the inner surfaces of porous materials that have small and deep pores using electrodeposition, metal layer joining, and electroless plating methods is difficult. Methods such as vacuum and ultrasonic mechanical processes are needed in addition, to uniformly coat metals onto the inner surfaces of CFms [16-20]. Alternatively, CFms have been uniformly embedded with copper via $CuSO_4$ solutions without the use of any mechanical process [21].

In this study, we investigate economical and convenient methods of preparing copper-nanoparticle-embedded CFms (Cu-CFms) using $CuSO_4$ solutions with different concentrations. The thermal and mechanical properties of the resulting Cu-CFms were investigated along with changes in the density and nanoparticulate size of the Cu.

Isotropic pitch (IP) (pyrolyzed fuel oil; GS Caltex, Seoul, Korea) with a softening point (SP) of 250°C was used as the carbon precursor for the CFms. Polyvinyl alcohol (PVA, 98%-99%, MW 30,000-50,000; Sigma-Aldrich, St. Louis, MO, USA) and acrylic acid (AAc, 99%; Sigma-Aldrich) were used as the hydrophilic polymer and organic compound, respectively, to prepare the hydrogel. Glutaraldehyde (GA, 25 wt% dissolved in water; Kanto Chemical,

Tokyo, Japan) and ethylene glycol dimethacrylate (EGDMA, 98%; Sigma-Aldrich) were used as cross-linking agents, and potassium persulfate (KPS, 99%; Sigma-Aldrich) was used as the radical initiator. Copper (II) sulfate ($CuSO_4$, 98%; Sigma-Aldrich) was used as the Cu source in the CFms for improving their mechanical strength and thermal conductivity. PVA (6 g) was dissolved in a 1 M NaOH solution (52 mL) at 140°C for 10 min. After the solution cooled, AAc (15 mL) and $CuSO_4$ (3.2, 4.8, or 6.6 g) were added; the resulting mixture was stirred for 30 min to dissolve and homogeneously disperse the $CuSO_4$ in the PVA-AAc solution. GA (1 mL), EGDMA (1.5 mL), and KPS (2 wt% dissolved in water, 1 mL) were added to the solution, and the resulting mixture was stirred for 3 min. The pitch (32 g, with particle sizes under 100 μm) was added to the prepared polymer solution containing $CuSO_4$, and additional $CuSO_4$ was added per weight of pitch at approximately 2.5, 3.7, and 5.0 w/w% weight conditions (polymers:pitch:$CuSO_4$ = 21.77:32.00:3.2-6.6 g); the resulting mixture was stirred for 1 h to completely mix the pitch. The mixture was formed to the slurry solution. The hydrogel containing the pitch and $CuSO_4$ was cured for 9 h at 60°C. The prepared gel was dried at 140°C for 13 h in air, and the dried gel was then heated to 600°C at 5°C/min and then isothermed at 600°C for 1 h to eliminate the polymers. The samples were subsequently carbonized under a nitrogen atmosphere at 1000°C using a heating rate of 5°C/min and an isotherm period of 1 h. The resulting samples were labeled as Pi, Pi-2.5Cu, Pi-3.7Cu, and Pi-5.0Cu to represent pitch, pitch-2.5 w/w% Cu, pitch-3.7 w/w% Cu, and pitch-5.0 w/w% Cu, respectively.

The thermal conductivity κ of the CFms was analyzed using the xenon flash diffusivity technique in an axial direction. The thermal diffusivity α was first measured for samples with dimensions of 12.5 × 12.5 × 3 mm^3 at 25°C, 100°C, 200°C, and 300°C using a LFA447 Nanoflash (Netzsch-Gerätebau GmbH, Selb, Germany). The thermal conductivities of at least three specimens were measured. The sample density ρ and the specific heat capacity C_ρ (0.831, 0.883, and 0.649 J/gK for Pi-2.5Cu, Pi-3.7Cu, and Pi-5.0Cu, respectively, and 1.0 J/gK for the Pi) were used to calculate the thermal conductivity of the samples according to the following equation (1):

$$\kappa = \alpha \cdot \rho \cdot C_\rho \quad (1)$$

The specific heat capacity was obtained from the analyzed values, such as thermal conductivity, thermal diffusivity, and density, using the above equation. The morphologies and bubble diameters [22] of the prepared Cu-CFms were analyzed using field-emission scanning electron microscopy (FE-SEM; S-4700, Hitachi, Tokyo, Japan) coupled with energy dispersive X-ray spectroscopy (EDS, EX-250; Horiba, Kyoto, Japan); this method allowed a point analysis of elemental composition over a focused region. The crystallinity of the Cu-CFms as a function of the Cu content used in their synthesis was analyzed using X-ray diffraction (XRD, D/MAX-2200 Ultima/PC; Rigaku, Tokyo, Japan). The porosity of samples was determined as both true and apparent densities by means of He. The true density was measured using an automatic gas pycnometer (Quantachrome/Ultrapycnometer 1200e, Quantachrome Instruments, USA). The compressive strengths of the CFms were measured using a micro materials tester (INSTRON 5848, 500N; INSTRON, Norwood, MA, USA) and a sample size of 3 × 3 × 3 mm^3. The compressive strengths of at least five samples were tested.

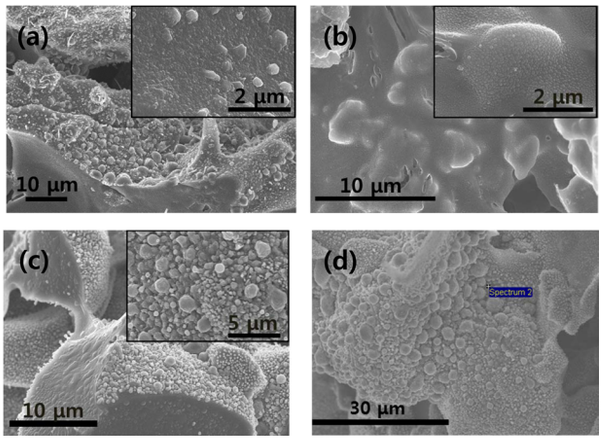

Fig. 1. Enlarged surface morphologies of the Cu-embedded carbon foams, (a) Pi-2.5Cu, (b) Pi-3.7Cu, (c) Pi-5.0Cu, and (d) image showing the location on Pi-5.0Cu at which energy dispersive X-ray spectroscopy analysis was performed.

The surface morphology of the CFm exhibited low roughness, with an average bubble diameter of 0.13 ± 0.07 mm. The Cu-CFms exhibited altered surface morphologies and bubble sizes. The bubble sizes of the Cu-CFms were 0.09 ± 0.04, 0.08 ± 0.04, and 0.08 ± 0.03 mm for Pi-2.5Cu, Pi-3.7Cu, and Pi-5.0Cu, respectively. The surface morphologies of the Cu-CFms exhibited an increase in roughness and a decrease of bubble size with increasing amounts of embedded Cu.

The inner surface morphologies of the Cu-CFms and the Cu nanoparticle sizes are shown in Fig. 1. The inner surface morphologies of the Cu-CFms are shown in Fig. 1a-c for three preparation methods: with Cu as commonly embedded on the inner surfaces of the CFms prepared from pitch, with $CuSO_4$, and with a polymer solution using a sacrificial template technique and heat treatment. The Cu nanoparticle sizes were 0.41 ± 0.06, 0.14 ± 0.00, and 1.00 ± 0.60 μm for Pi-2.5Cu, Pi-3.7Cu, and Pi-5.0Cu, respectively. The Cu nanoparticle sizes increased with increasing $CuSO_4$ concentration. However, the Cu nanoparticle size of Pi-3.7Cu was significantly reduced because the $CuSO_4$ was highly dispersed in the CF at this concentration. The Cu nanoparticle sizes and their dispersion were controlled via the $CuSO_4$ concentration.

In addition, the Cu nanoparticles were typically embedded on the inner and outer surfaces of the CFms; thus, CFms were not formed when the $CuSO_4$ concentration exceeded Pi-5.0Cu because of the presence of non-binding pitch.

Elemental analysis of the Cu-CFms was performed by EDS at the selected zone indicated in Fig. 1d. The elemental percentages of C, O, Na, K, and Cu in Pi-5.0Cu are reported to be 11.59, 3.94, 3.54, 0.05, and 80.89, respectively.

The crystal structures of the pristine and Cu-CFms were analyzed by XRD, and the results are shown in Fig. 2. Pi was the reference material as a non-treated CFm; its XRD pattern displayed carbon crystalline peaks at 2θ = 26° and 43°, which were indexed as 002 and 101, respectively. The pattern of Pi-2.5Cu exhibited peaks at 2θ = 44°, 52°, and 74°, which were attributed

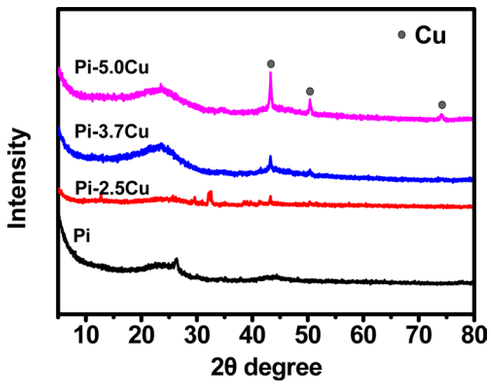

Fig. 2. X-ray diffraction patterns of the pristine and Cu-embedded carbon foams.

to the 111, 200, and 220 reflections of poorly crystalline Cu, respectively [11]. It also contained a peak at 2θ = 31° associated with the 211 reflection of crystalline Na_2SO_4, which formed via a side reaction between NaOH and $CuSO_4$ [10]. The intensities of the crystalline Cu peaks substantially increased with increasing amounts of Cu in the CFms from Pi-2.5Cu to Pi-5.0Cu.

The Cu-CFms were prepared with different $CuSO_4$ concentrations using heat treatment. The various concentrations resulted in different thermal conductivities and compressive strengths, as a consequence of the apparent density and different nanoparticle sizes of Cu, which embedded different amounts of Cu in the CFms. The Cu was possibly embedded via adhesion with carbon in the CFms, leading to improved thermal conductivity and compressive strength as the density varied [12,14].

The thermal conductivities and compressive strengths of the CFm and Cu-CFms are shown in Table 1 and Fig. 3a and b. Pi was the non-treated CFm used as a reference material; it exhibited a thermal conductivity of 2.50 ± 0.00 W/mK and a compressive strength of 8.05 ± 1.72 MPa at a low apparent density of 0.69 g/cm^3. The thermal conductivities and compressive strengths of the Pi-2.5Cu, Pi-3.7Cu, and Pi-5.0Cu were 3.86 ± 0.00, 1.98 ± 0.04, and 1.61 ± 0.05 W/mK and 10.04 ± 4.46, 4.52 ± 0.82, and 2.98 ± 0.14 MPa, respectively, with apparent densities of 0.83, 0.47, and 0.61 g/cm^3. The increased amounts of Cu in the CFms inhibited the pitch binding strength, leading to reduced apparent densities of the Cu-CFms with increasing $CuSO_4$ concentration. The dependence of pitch binding strength on Cu contents could be confirmed by the bubble sizes and the enlarged inner and outer surface morphologies of the CFms. The bubble sizes of the Cu-CFms were further increased with increasing amounts of Cu content. Also, Cu nanoparticles were

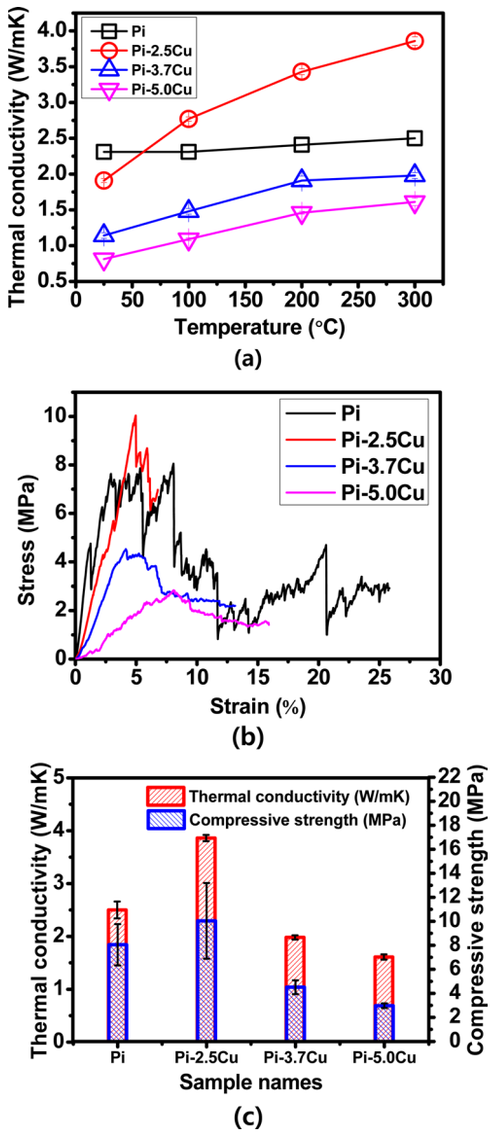

Fig. 3. Mechanical properties of the pristine and Cu-embedded carbon foams, thermal conductivity (a), compressive strength (b), and relations of mechanical properties (c).

embedded on the inner surface and pore walls of the CFms with increasing $CuSO_4$ concentration.

The relationships between the thermal conductivity and compressive strength of the prepared samples and their appar-

Table 1. Mechanical properties of the pristine and Cu-embedded carbon foams

	Pi	Pi-2.5Cu	Pi-3.7Cu	Pi-5.0Cu
Compressive strength (MPa)	8.05	10.04	4.52	2.98
Thermal conductivity (W/mK)	2.50	3.86	1.98	1.61
True density (g/cm^3)	1.49	1.77	1.74	1.84
Apparent density (g/cm^3)	0.69	0.83	0.47	0.61

Table 2. Mechanical properties of carbon foams with Cu

Sample	Density (g/cm^3)	Thermal conductivity (W/mK)	Compressive strength (MPa)	Reference
Copper-graphite composite	-	20-21	-	[7]
Copper plating on CFms	-	-	0.70-1.66	[8]
Cu-coated CFms	-	8-180	4.5-8.6	[22]
IP-based Cu-CFms	0.47-0.69	1.61-3.08	2.98-10.04	This work

CFms, carbon foams; IP, isotropic pitch.

ent density are shown in Fig. 3c. The thermal conductivity and compressive strength of the prepared samples decreased with decreasing apparent density. In addition, the nanoparticle sizes of the Cu affected the thermal conductivity of the Cu-CFms; the nanoparticle sizes of the Cu in the CFms were 0.41 ± 0.06, 0.14 ± 0.00, and 1.0 ± 0.60 μm for Pi-2.5Cu, Pi-3.7Cu, and Pi-5.0Cu, respectively. The thermal conductivity reached its highest value of 362 W/mK when the Cu nanoparticle size exceeded 0.4 μm; this thermal conductivity was in the range of the thermal conductivity of the Cu-CFms with Cu nanoparticle sizes of 0-0.5 μm because of the effect of particle size on the thermal conductivity of the nanofluids. The effect of particle size on the thermal conductivity was governed by the temperature-thermal conductivity behavior of the base thermal fluids; the effective thermal conductivity of the nanofluids decreased with the decreasing size of dispersed particles below a critical particle size [23]. The results showed that thermal conductivity and compressive strength were affected by the apparent density as well as the amounts and nanoparticle size of the Cu in the CFms. Pi-2.5Cu exhibited increases in thermal conductivity and compressive strength of approximately 54.40% and 24.72%, respectively, compared to those of the non-treated CFm.

The physical properties of various CFms with Cu are shown in Table 2. The CFms with Cu reported in the table were prepared by various methods, such as composite formation, plating, coating, and embedding. According to the results in Table 2, the thermal and mechanical properties of CFms with Cu were also changed depending on the methods and precursors used in their preparation.

The Cu-CFms prepared in this work exhibited increased thermal conductivity and compressive strength because of the high thermal conductivity and mechanical strength of the Cu. The IP-based Cu-CFms exhibited low thermal conductivity, in the range of 1.61-3.08 W/mK, because of the use of IP, which exhibits low thermal conductivity due to its poorly developed crystalline structure. Nonetheless, the thermal conductivity of these Cu-CFms was 54.40% greater than that of the non-treated CFm.

However, the Cu-CFms exhibited a high compressive strength range of 2.98-10.04 MPa because the Cu was strongly adhered to the carbon materials, and reduced cracking by serving as a filler. As a result, the Cu-CFms prepared in this work exhibited a compressive strength 24.72% greater than that of the non-treated CFm. In addition, the compressive strength of the samples prepared in this work exhibited the highest values among the CFms with Cu samples reported in Table 2.

Cu-CFms were prepared using different $CuSO_4$ concentrations via heat treatment; the variation of the $CuSO_4$ concentration affected the thermal conductivity and compressive strength of the resulting CFms and the size of the Cu nanoparticles. The thermal conductivity and compressive strength of the CFms were affected by the apparent density as well as the amount and nanoparticle size of the Cu in the CFms. The apparent densities of the CFms were reduced with increases in the bubble sizes and the amount of Cu in the CFms, which inhibited the pitch binding strength. As a consequence, Pi-2.5Cu exhibited the highest thermal conductivity and compressive strength at 3.86 ± 0.00 W/mK and 10.04 ± 4.46 MPa, respectively, with an apparent density of 0.83 g/cm^3. These values represent increases in thermal conductivity and compressive strength of approximately 54.40% and 24.72%, respectively, compared to those of the non-treated CFm.

In addition, the Cu nanoparticle size played an important role in increasing the thermal conductivity of the CFms. The highest thermal conductivity was achieved in the case of Pi-2.5Cu, whose Cu nanoparticles were 0.41 ± 0.06 μm in diameter.

Conflict of Interest

No potential conflict of interest relevant to this article was reported.

References

[1] Calvo M, García R, Arenillas A, Suárez I, Moinelo SR. Carbon foams from coals: a preliminary study. Fuel, **84**, 2184 (2005). http://dx.doi.org/10.1016/j.fuel.2005.06.008.

[2] Liu H, Li T, Wang X, Zhang W, Zhao T. Preparation and characterization of carbon foams with high mechanical strength using modified coal tar pitches. J Anal Appl Pyrolysis, **110**, 442 (2014). http://dx.doi.org/10.1016/j.jaap.2014.10.015.

[3] Park MS, Lee SE, Kim MI, Lee YS. CO_2 adsorption characteristics of slit-pore shaped activated carbon prepared from cokes with high crystallinity. Carbon Lett, **16**, 45 (2015). http://dx.doi.org/10.5714/CL.2015.16.1.045.

[4] Sanchez-Coronado J, Chung DDL. Thermomechanical behavior of a graphite foam. Carbon, **41**, 1175 (2003). http://dx.doi.org/10.1016/s0008-6223(03)00025-3.

[5] Singh M, Asthana R, Smith CE, Gyekenyesi AL. Integration of Cu-clad-Mo to high conductivity graphite foams. Curr Appl Phys, **12**, S116 (2012). http://dx.doi.org/10.1016/j.cap.2012.02.033.

[6] Choi JY, Park SJ. Effect of manganese dioxide on supercapacitive behaviors of petroleum pitch-based carbons. J Ind Eng Chem, **29**,

408 (2015). http://dx.doi.org/10.1016/j.jiec.2015.04.022.

[7] Johnson MT, Childers AS, Ramírez-Rico J, Wang H, Faber KT. Thermal conductivity of wood-derived graphite and copper-graphite composites produced via electrodeposition. Compos Part A Appl Sci Manuf, **53**, 182 (2013). http://dx.doi.org/10.1016/j.compositesa.2013.06.009.

[8] Zhai L, Liu X, Li T, Feng Z, Fan Z. Vacuum and ultrasonic co-assisted electroless copper plating on carbon foams. Vacuum, **114**, 21 (2015). http://dx.doi.org/10.1016/j.vacuum.2014.12.005.

[9] Isani G, Falcioni ML, Barucca G, Sekar D, Andreani G, Carpenè E, Falcioni G. Comparative toxicity of CuO nanoparticles and $CuSO_4$ in rainbow trout. Ecotoxicol Environ Saf, **97**, 40 (2013). http://dx.doi.org/10.1016/j.ecoenv.2013.07.001.

[10] Mishra A, Dwivedi J, Shukla K, Malviya P. X-Ray diffraction and Fourier transformation infrared spectroscopy studies of copper (II) thiourea chloro and sulphate complexes. J Phys Conf Ser, **534**, 012014 (2014). http://dx.doi.org/10.1088/1742-6596/534/1/012014.

[11] Han MS, Lee BG, Ahn BS, Moon DJ, Hong SI. Surface properties of $CuCl_2$/AC catalysts with various Cu contents: XRD, SEM, TG/DSC and Co-TPD analyses. Appl Surf Sci, **211**, 76 (2003). http://dx.doi.org/10.1016/S0169-4332(03)00177-6.

[12] Schrank C, Schwarz B, Eisenmenger-Sittner C, Mayerhofer K, Neubauer E. Influence of thermal treatment on the adhesion of copper coatings on carbon substrates. Vacuum, **80**, 122 (2005). http://dx.doi.org/10.1016/j.vacuum.2005.07.031.

[13] Bittencourt C, Ke X, Van Tendeloo G, Thiess S, Drube W, Ghijsen J, Ewels CP. Study of the interaction between copper and carbon nanotubes. Chem Phys Lett, **535**, 80 (2012). http://dx.doi.org/10.1016/j.cplett.2012.03.045.

[14] Guo R, Zhen W, Pan W, Zhou Y, Hong J, Xu H, Jin Q, Ding CG, Guo SY. Effect of Cu doping on the SCR activity of CeO_2 catalyst prepared by citric acid method. J Ind Eng Chem, **20**, 1577 (2014). http://dx.doi.org/10.1016/j.jiec.2013.07.051.

[15] Thouchprasitchai N, Luengnaruemitchai A, Pongstabodee S. Water-gas shift reaction over Cu–Zn, Cu–Fe, and Cu–Zn–Fe composite-oxide catalysts prepared by urea-nitrate combustion. J Ind Eng Chem, **19**, 1483 (2013). http://dx.doi.org/10.1016/j.jiec.2013.01.012.

[16] Zhao Z, Wang X, Qiu J, Lin J, Xu D, Zhang C, Lv M, Yang X. Three-dimentional graphene-based hydrogel/aerogel materials. Rev Adv Mater Sci, **36**, 137 (2014).

[17] Xu Y, Sheng K, Li C, Shi G. Self-assembled graphene hydrogel via a one-step hydrothermal process. ACS Nano, **4**, 4324 (2010). http://dx.doi.org/10.1021/nn101187z.

[18] Hu H, Zhao Z, Gogotsi Y, Qiu J. Compressible carbon nanotube-graphene hybrid aerogels with superhydrophobicity and superoleophilicity for oil sorption. Environ Sci Technol Lett, **1**, 214 (2014). http://dx.doi.org/10.1021/ez500021w.

[19] Almajali M, Lafdi K, Prodhomme PH, Ochoa O. Mechanical properties of copper-coated carbon foams. Carbon, **48**, 1604 (2010). http://dx.doi.org/10.1016/j.carbon.2009.12.060.

[20] Lafdi K, Almajali M, Huzayyin O. Thermal properties of copper-coated carbon foams. Carbon, **47**, 2620 (2009). http://dx.doi.org/10.1016/j.carbon.2009.05.014.

[21] Kumar R, Kumari S, Dhakate SR. Nickel nanoparticles embedded in carbon foam for improving electromagnetic shielding effectiveness. Appl Nanosci, **5**, 553 (2015). http://dx.doi.org/10.1007/s13204-014-0349-7.

[22] James L, Austin S, Moore CA, Stephens D, Walsh KK, Dale Wesson G. Modeling the principle physical parameters of graphite carbon foam. Carbon, **48**, 2418 (2010). http://dx.doi.org/10.1016/j.carbon.2010.02.043.

[23] Warrier P, Teja A. Effect of particle size on the thermal conductivity of nanofluids containing metallic nanoparticles. Nanoscale Res Lett, **6**, 247 (2011). http://dx.doi.org/10.1186/1556-276X-6-247.